Freeze-dried chitosan/PRP implants improve marrow stimulated cartilage repair in a chronic defect rabbit model

Dwivedi G[1], Chevrier A[2], Hoemann CD[1, 2] and Buschmann MD[1, 2]

[1]Biomedical Engineering Institute and [2]Chemical Engineering Department, Ecole Polytechnique, Montreal, QC, Canada

Corresponding author: Prof Michael D. Buschmann, Department of Chemical Engineering, Ecole Polytechnique, PO Box 6079 Succ Centre-Ville, Montreal, Quebec, Canada, H3C 3A7, Fax: 514 340 2980 Tel: 514 340 4711 ext. 4931, E-mail: michael.buschmann@polymtl.ca

Running title: Chitosan/PRP for cartilage repair in a chronic model

Author contributions statement: All authors made substantial contributions to research design, acquisition, analysis and interpretation of data, drafting and revision of the paper. All authors have read and approved the final submitted manuscript.

Keywords: Cartilage repair, Marrow stimulation, Chronic model, Chitosan, Platelet-rich plasma

Role of funding source: This work was supported by the Canadian Institutes of Health Research, Canada Foundation for Innovation, Groupe de Recherche en Sciences et Technologies Biomédicales, Natural Sciences and Engineering Research Council of Canada and Ortho Regenerative Technologies Inc.

Abstract

Purpose

Bone Marrow Stimulation (BMS) improves knee joint function but elicits incomplete repair. Liquid chitosan (CS)-glycerol phosphate/blood clots have been shown to improve BMS-based cartilage repair. Platelet-rich-plasma (PRP) – a rich source of growth factors and cytokines - improves recruitment and chondrogenic potential of subchondral mesenchymal stem cells. We hypothesized that repair response in a rabbit chronic defect model will improve when freeze-dried chitosan/PRP is used to augment BMS.

Methods

Bilateral trochlear defects created in New Zealand White rabbits were allowed to progress to a chronic stage over 4 weeks. Chronic defects were debrided and treated by BMS in second surgery, then augmented with PRP (BMS+PRP) or chitosan-PRP implants (BMS+CS/PRP). The quality of 8 week repair tissue was assessed by macroscopic, histological and micro-CT analysis.

Results

ICRS macroscopic scores indicated fibrocartilaginous or fibrous repair in control defects that were improved in the BMS+CS/PRP group. An overall improvement in repair in BMS+CS/PRP

group was further confirmed by higher O'Driscoll scores, %Saf-O and %Coll-II values. Micro-CT analysis of subchondral bone indicated on-going remodeling with repair still underway.

Conclusion

Quality and quantity of cartilage repair was improved when chitosan/PRP implants were used to augment BMS in a chronic defect model.

Introduction

Bone marrow stimulation (BMS) is a purely surgical process which initiates cartilage repair by fracturing or drilling into subchondral bone. BMS procedures initiate the formation of a blood clot around fractured bone followed by migration of subchondral progenitor cells which differentiate into a chondrogenic phenotype to form a repair tissue with variable amounts of hyaline and fibrous cartilage [1]. The repair tissue is typically characterized by low quality and compromised durability, and larger lesions in older patients are even more challenging to treat.

One possible reason for the poor performance of BMS is that the blood clot rapidly shrinks to a fraction of its initial size due to platelet-mediated clot retraction, resulting in lack of defect filling and possible detachment from the tissue surface. One way to prevent clot retraction is to add chitosan (CS), a polymer of glucosamine and N-acetyl glucosamine units, to the blood [2]. Liquid CS-glycerol phosphate (GP)/blood implants can be applied over BMS-treated cartilage defects where they coagulate *in situ* and inhibit platelet-mediated clot retraction leading to the formation of a voluminous, adherent and physically stable clot with access to underlying marrow [3]. When used in conjunction with BMS procedures, CS-GP/blood implants promote cell recruitment, transient vascularization and subchondral bone remodeling leading to integrated repair and increased hyaline character of the repair tissue [2-5]. These implants were tested clinically [6, 7] and have now been approved in several countries to treat cartilage lesions (BST-CarGel®, Smith and Nephew, USA). One drawback of this technology is that liquid CS solutions have limited stability during storage due to acid hydrolysis of CS and loss of viscosity

[8]. A freeze–dried form of CS would not only overcome this limitation by increasing stability and shelf life but also permit easier sterilization.

A microenvironment stimulating chondrogenic differentiation of marrow-derived mesenchymal stem cells (BMSCs) may be achieved by addition of platelet-rich-plasma (PRP) to the defect milieu. PRP is prepared by sequential centrifugation of whole blood and is a rich source of growth factors and cytokines such as PDGF, VEGF, IGF, EGF etc which play an important role in inflammatory and wound repair phenomena [9-11]. Earlier studies have shown that PRP can induce a significant improvement in BMSC recruitment, angiogenesis [12, 13], expression of cartilage matrix [14], proliferation and viability of chondrocytes and BMSCs [15-16] as well as stimulate migration and chondrogenic potential of subchondral BMSCs [17]. Using an ovine chronic defect model, Milano *et al* showed that when used as an adjunct to BMS, PRP enhanced the repair response versus BMS alone [18]. Although the application of PRP improved the macroscopic and mechanical outcome, the hyaline nature of the repair tissue was still lacking. The efficacy of PRP in improving cartilage repair has been questioned due to multiple studies reporting less positive results in animal models [19-22]. We believe that inferior outcome with PRP could arise from the poor stability of PRP clots *in vivo*, which is even more pronounced than blood clots [23]. Combination of PRP with CS may help in overcoming this limitation thereby increasing residency and bioactivity of PRP.

Progression to advanced stages of osteoarthritis (OA) may be prevented by early diagnosis and treatment. However, in cartilage lesions that are asymptomatic for longer times [24,25], BMS may have more severe limitations and therefore be less effective in treating older, chronic

and extensive lesions. Chronic defects may alter joint homeostasis resulting in less favourable clinical outcomes [26-28]. To better represent this clinical situation, we developed a pre-clinical model to simulate degenerated chronic defects and examine the potential of BMS combined with CS/PRP in improvement of cartilage regeneration in chronic defects that are more challenging than acute lesions. It is already known that osteochondral defects smaller than 3 mm in young rabbits possess the potential for spontaneous regeneration [29] and several studies have reported a period of approximately 1 month to be adequate for development of chronic defect model in small animals [30,31]. Accordingly, we used skeletally mature rabbits with a defect size of 4 × 4 mm developed to chronicity over a period of four weeks. With these aspects in mind we carried out this study to test the hypothesis that augmentation of BMS with freeze-dried CS/PRP implants would improve repair response in a rabbit chronic defect model compared to BMS augmented with recalcified PRP.

Materials and Methods

Preparation of freeze-dried chitosan formulation and PRP isolation

Freeze-dried CS cakes consisted of 0.56% (w/vol) CS with 1% (w/vol) trehalose and 42.2 mM calcium chloride. To prepare, 0.056 g CS (Number average molar mass M_n 36.6 kDA and 80.2% DDA, produced in-house and characterized with NMR spectroscopy [32] and size-exclusion chromatography/multi-angle laser light scattering [33]) was mixed with 7.69 g water and 156 µl of 1 N HCl. Following overnight mixing, 1.56 ml of 3% (w/w) $CaCl_2$ and 666 µl of 15% (w/v) trehalose solutions were added and the final solution was sterilized by filtration. Finally, 300 µl aliquots were prepared in 2 ml sterile glass vials and freeze-dried using the following conditions: 1) Ramped freezing to -40°C in 1 hour then isothermal 2 hours at -40°C, 2) -40°C for 48 hours at 100 millitorrs and 3) Ramped heating to 30°C in 12 hours then isothermal 6 hours at 30°C, at 100 millitorrs.

Autologous PRP was generated by sequential centrifugation of citrate-anticoagulated whole blood. Approximately 9 ml of autologous blood was extracted from rabbit and mixed with 1 ml of 3.8% (w/vol) sodium citrate before further processing. The whole blood was centrifuged at 160g for 10 minutes. Following collection of the supernatant in addition to approximately the first 1-2 mm of erythrocytes, a second centrifugation was carried out at 400g for 10 minutes. Bottom 1.5 ml fraction containing PRP was isolated. Complete blood counts revealed that, on average, the ratio of platelets, leukocytes and erythrocytes in isolated PRP versus whole blood was 3X, 1X and 0.1X, respectively, which makes this a leukocyte-rich PRP.

Experimental design and rabbit surgical model for cartilage repair in chronic lesions

Canadian Council on Animal Care guidelines were observed and research protocol was approved by an institutional ethics committee for animal research. Using skeletally mature female New Zealand White rabbits, the chronic defect model was first validated in a pilot study utilizing a small number of animals (n=3) and short duration (4 weeks development to chronicity followed by 3 weeks repair). The objective was to assess the feasibility of development of the model as well as compare fresh chronic defects (n=2 knees) to chronic defects after 4 weeks development (n=2 knees) and repair responses induced in chronic defects by BMS alone (n=1 knee) and BMS augmented with 1% (w/v) CS/PRP implants (n=1 knee). PRP controls were not included in this pilot study since the aim was to validate the chronic model rather than study the effect of treatments.

A larger group (n=8) of skeletally mature (8-9 months old) female New Zealand White rabbits were then used in a bilateral model that limits the influence of inter-animal variation via a contralateral control. Two surgeries were performed to assess the development and repair of chronic cartilage defects. Following induction with xylazine-ketamine, animals were maintained under general anaesthesia using isofluorane-oxygen. Bilateral, parapatellar arthrotomies were performed to expose the synovial joint. Full-thickness chondral lesions measuring 4 × 4 mm were created in the trochlear central groove by scraping with 1.5 and 2.75 mm flat surgical blades taking care not to remove calcified cartilage. Knees were closed in sutured layers. A second surgery was performed four weeks later and the original lesion identified. Calcified

cartilage (CC) and repair tissues (when present) were completely debrided using a flat blade to expose the underlying subchondral bone, without damaging the subchondral bone plate. Using a high speed microdrill, four subchondral perforations measuring 0.9 mm diameter and 6 mm deep were made on each trochlear defect in both knees, similar to what was done previously by our group in acute models [34,35]. Constant cooling irrigation was applied for removal of loose bone debris and prevention of heat necrosis [36]. The defect on one knee received treatment with one drop of CS/PRP mixture. Immediately before implantation, the CS cake (300 µL) was solubilized with 300 µL autologous PRP. One drop of CS/PRP was applied to the drilled trochlear defect using a 1 ml syringe and 18 gauge needle. The contralateral defect was treated with one drop of PRP recalcified with 42.2 mM calcium chloride. In both cases, knees were closed five minutes post application. The treatments were alternated between right and left knees [Fig. 1]. The patella was repositioned and knee was closed in sutured layers. No perioperative antibiotics were administered after either surgery but animals received extended analgesia with a fentanyl transdermal patch. Knees were allowed unrestricted motion and constantly monitored for infections and other complications following both surgeries. Animals were sacrificed eight weeks later and knees were harvested for comparison of marrow stimulated repair response in presence of CS/PRP (BMS+CS/PRP group, n=8 knees) and recalcified PRP (BMS+PRP group, n=8 knees).

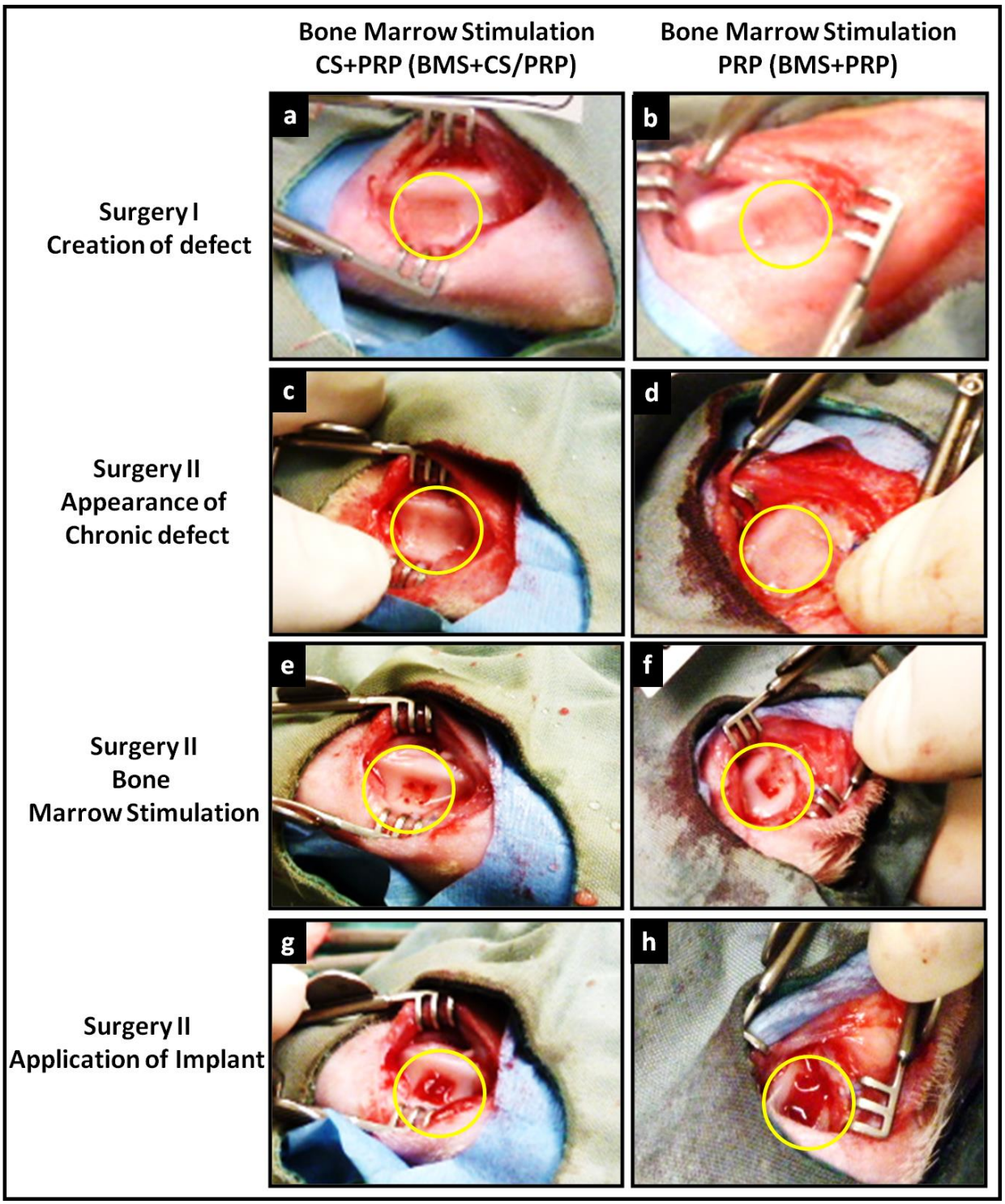

Fig. 1: Procedure of surgical manipulation to create and treat chronic defects using BMS+CS/PRP implants (left panels) or BMS+PRP (right panels). a,b: Creation of 4 × 4 mm

defects by debriding all non-calcified cartilage from trochlea; c,d: Appearance of chronic defects four weeks after creation at the time of second surgery; e,f: Treatment of defects by debriding spontaneous repair tissue (when present) and calcified cartilage and drilling 4 holes measuring 0.9 mm in width and 6 mm deep; g: Application of CS/PRP implant at defect site; h: Application of recalcified PRP at defect site.

Characterization of repair

Animals were sacrificed by overdose of pentobarbital and femoral ends were fixed in 4% paraformaldehyde /1%glutaraldehyde /0.1M Sodium cacodylate (pH 7.3). Low magnification images of fixed repair tissues were obtained with a dissection microscope equipped with digital camera to determine their gross structure and appearance using Northern Eclipse software (Empix Imaging). Images of repair tissues were scored by two independent, blinded readers using the ICRS macroscopic scoring system (ranging from 0, for severely abnormal to 12, for normal) [37]. Scores from two readers were averaged and used as an indicator of gross pathology of repair tissues.

Samples were decalcified in EDTA with trace paraformaldehye and embedded in OCT and transverse sections were obtained from three levels: from the middle of the proximal and distal holes and from between holes. Sections were stained with Safranin O/Fast Green and scanned using a Nanozoomer RS system (Hamamatsu, Japan). Repair tissue was defined as all non-mineralized tissue above the subchondral bone plate. Digital Saf-O stained sections were scored by two independent, blinded observers using a previously published O'Driscoll histological

scoring method (ranging from 0, for worst tissue quality to 27, for best tissue quality) modified to assess subchondral bone health by an additional 3 point value [5]. Each Saf-O stained section was assessed for 10 criteria (fig. 6c) to evaluate quality of repair tissue in addition to health of adjacent cartilage and subchondral bone repair. The scores obtained from three sections were averaged for both readers and used for assessment of quality of fill in defects (ICC of 0.86 for total O'Driscoll score for both readers).

Sections collected from each defect were also used to determine %Saf-O and %Coll-II in the chondral repair tissue using a previously described method [38]. Briefly, soft repair tissues were cropped by identifying projected articular surface and tidemark with the help of flanking articular cartilage and accounting for the curvature of the trochlear groove. Only the soft repair tissue above the tidemark was used to determine hue-saturation-value threshold limits for Saf-O and Coll-II. %Saf-O and %Coll-II positive region of repair tissues were measured using in-house Matlab routine software.

MicroCT analysis of subchondral bone repair

Micro CT scanning of fixed femur ends was done to characterize subchondral bone repair and remodelling (Skyscan x-ray microtomography 1172, Kontich, Belgium). Femurs were scanned with an aluminium filter at 14.1 µM pixel size resolution with an X-ray source voltage of 56 kV, 1180 BMSec exposure, 0.45 rotation steps and 3 averaging frames. Trochlear micro CT image stacks were first reconstructed with NRecon software 1.6.1.5 using the following parameters: Smoothing of 2, Ring artifact reduction of 10, Beam hardening correction of 40%.

Datasets were repositioned with DataViewer software 1.4.3 and region of interest were applied followed by 3D micro CT analysis. The regions of interest were of the rectangle adapted surface type [39] and measured 3 mm X 3 mm X 2 mm [Fig. 1S]. Bone morphometric parameters were calculated including bone surface density (BS/TV), bone surface (BS), bone volume (BV), porosity, connectivity density and number and thickness of trabeculae, by using the global thresholding procedure in CTAn software (version 1.9.3.0, Skyscan, Kontich, Belgium).

Statistical Analysis

Statistical analyses were performed using SAS Enterprise Guide 7.1 and SAS 9.4. Since several sections were collected from both legs of each rabbit, a mixed model was used to account for the influence of donor. Fixed effects were treatments (BMS+PRP, n=8 knees and BMS+CS/PRP, n=8 knees), while donor was a random effect. Data in figures are presented as mean (diamond); median (line); Box: 25th and 75th percentile; Whiskers: Box to the most extreme point within 1.5 interquartile range. $p<0.05$ was considered statistically significant.

Results

Freeze dried chitosan/PRP implants induced inflammatory and wound bloom repair responses in chronic cartilage defects

Although debridement appeared to have preserved the calcified cartilage intact due to absence of any punctuate bleeding at the time of initial surgery [Fig. 1a,b], the histological examination of Saf-O stained transverse sections of fresh defects showed that calcified cartilage had been partly debrided [Fig. 2e,i]. Chronic defects were noticeably distinct from the surrounding healthy tissue after 4 weeks [Fig. 1c,d], and residual calcified cartilage along with spontaneous repair response arising from the bone was occasionally observed [Fig. 2f,j]. Complete debridement down to subchondral bone was performed prior to BMS [Fig. 1e,f] and application of either CS/PRP [Fig. 1g] or recalcified PRP [Fig. 1h].

Defects treated with BMS+CS/PRP showed incomplete repair at 3 weeks [Fig. 2c] and histological examination of Saf-O stained transverse sections taken through holes revealed depressed repair tissues and enlarged remodeling drill holes [Fig. 2g,k], reminiscent of a wound bloom repair response [23]. Drill holes were devoid of subchondral cartilage and mostly filled with a polymorphonuclear cell-rich granulation tissue, where neutrophils colocalized with CS [Fig. 2g,k]. Contralateral defects treated with BMS alone also demonstrated incomplete repair at 3 weeks [Fig. 2d] and histological examination showed fibrocartilaginous and endochondral ossification repair responses, associated with chondrocyte hypertrophy and vascular invasion [Fig. 2h,l].

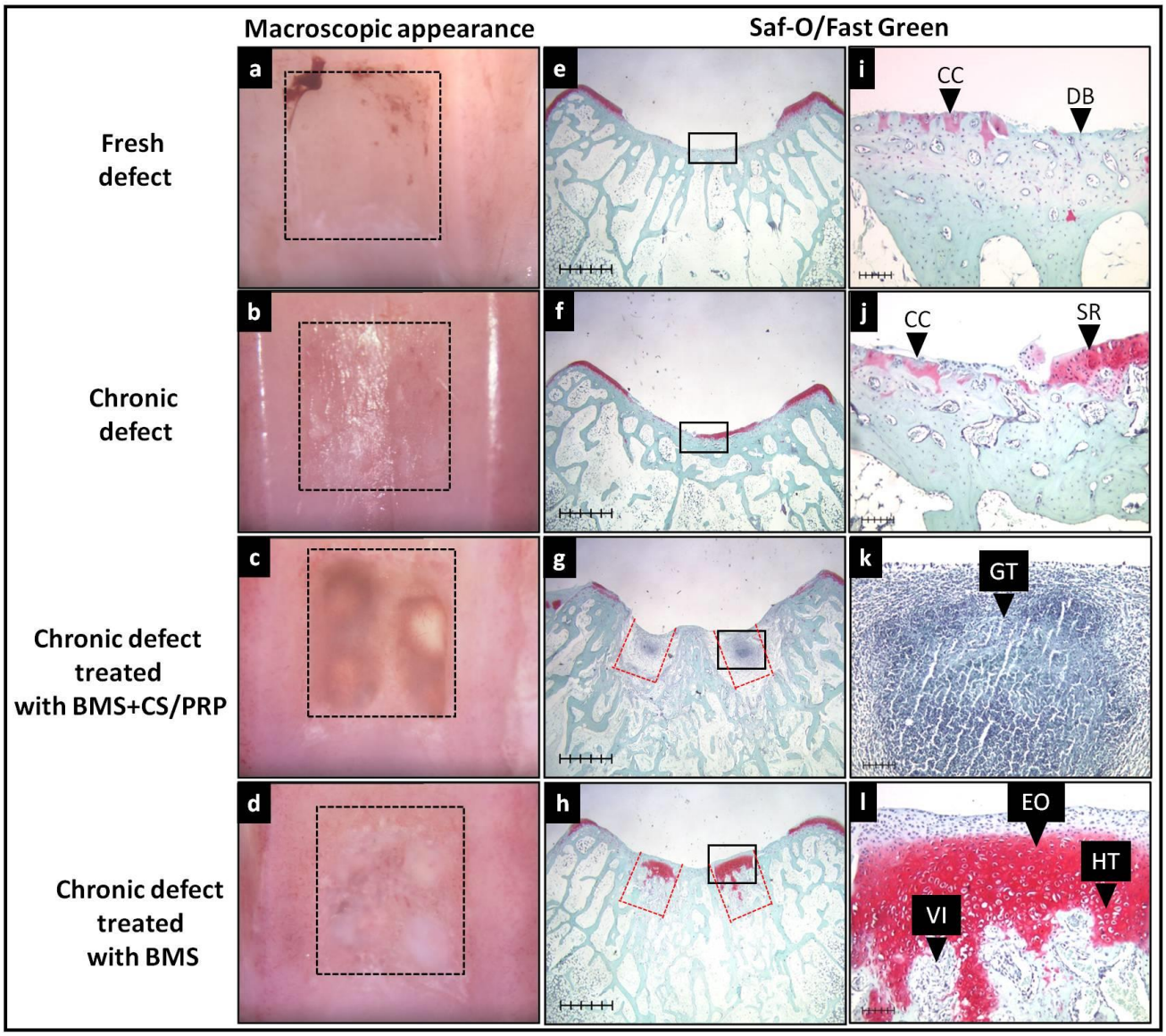

Fig. 2: Macroscopic and histopathological assessment of fresh defect (a,e,i), chronic defect after 4 weeks development (b,f,j), chronic defect treated with BMS+CS/PRP implant (c,g,k) and chronic defect treated with BMS alone (d,h,l). (e,i): Debridement was not homogenous and varying levels of calcified cartilage (CC) and debrided bone (DB) were seen in freshly debrided defects. (f,j): After 4 weeks, chronic defects showed evidence of partial spontaneous repair (SR)

in some areas along with tufts of calcified cartilage (CC). (g,k): Granulation tissue formation (GT) and enlarged drill holes were seen in presence of CS/PRP implants. (h,l): Fibrocartilagenous repair and endochondral ossification (EO) process were seen in presence of BMS alone, associated with chondrocyte hypertrophy (HT) and vascular invasion (VI). Red dotted lines in g & h represent original drill holes- hole enlargement and wound bloom effect is apparent in defect treated with BMS+CS/PRP (g). Scale bar (e-h):1 mm, (i-l): 100 µm.

Chitosan/PRP implants solidified quickly *in situ* and improved the macroscopic repair appearance in chronic defects

Clear differences in the solidification and stability of implants were observed at the time of surgery. On average, CS/PRP implants solidified *in situ* within 30-60 seconds. In contrast, in most cases, recalcified PRP implants did not coagulate even after passage of 5 minutes. In general, assessment of 8 week repair outcome was found to be generally poor [Fig. 3], most likely due to the chronic nature of the current defects. Incomplete fill and poor repair tissue integration to adjacent cartilage tissue were observed in both groups [Fig. 3]. Defect surfaces were significantly depressed with irregular surface [Fig. 3]. Appearance of repair tissues varied from dense white, glossy to reddish, spongy or tufty [Fig. 3]. Although higher for BMS+CS/PRP group (Mean score 4.75 ± 2.25) compared to BMS+PRP group (Mean score 3.25 ± 2.05), macroscopic ICRS scores did not show a significant difference between treatments ($p=0.16$) [Fig. 3e].

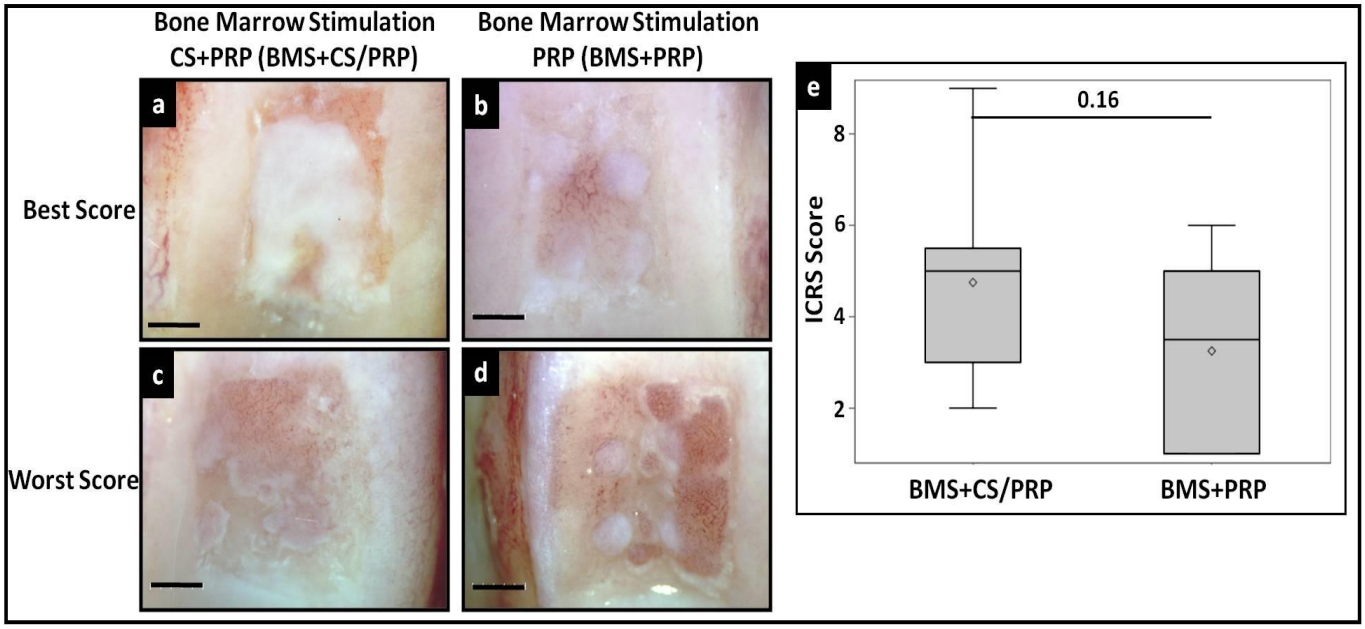

Fig. 3: Best (a,b) and worst (c,d) repair response in defects treated with BMS+CS/PRP (a,c) and BMS+PRP (b,d). Scale bar=1 mm. (e): Mean macroscopic ICRS score was higher (non-significant) in defects treated with BMS+CS/PRP versus defects treated with BMS+PRP.

However, the BMS+CS/PRP group had the only instance of a nearly normal (grade II) repair response and only two severely abnormal (grade IV) repair outcomes, while the BMS+PRP group had 4 instances each of abnormal (grade III) and severely abnormal (grade IV) outcomes [Table 1].

Table 1: Number of defects in each repair category for both treatments. Macroscopic repair scored according to the ICRS system.

Grade of repair	BMS+CS/PRP	BMS+PRP
I (12-Normal)	0	0
II (8-11 Nearly Normal)	1	0
III (4-7 Abnormal)	5	4
IV (1-3 Severely Abnormal)	2	4

Histological assessment showed superior repair in defects treated with chitosan/PRP implants

Higher expression of GAGs and type II collagen was observed in defects with the best histological scores [Fig.4 a,b,i,j,e,f,m,n], compared to defects with lowest scores [Fig.4 c,d,k,l,g,h,o,p]. Where present, repair tissues showed good integration to underlying bone, although bonding with adjacent cartilage was poor in both groups [Fig.4].

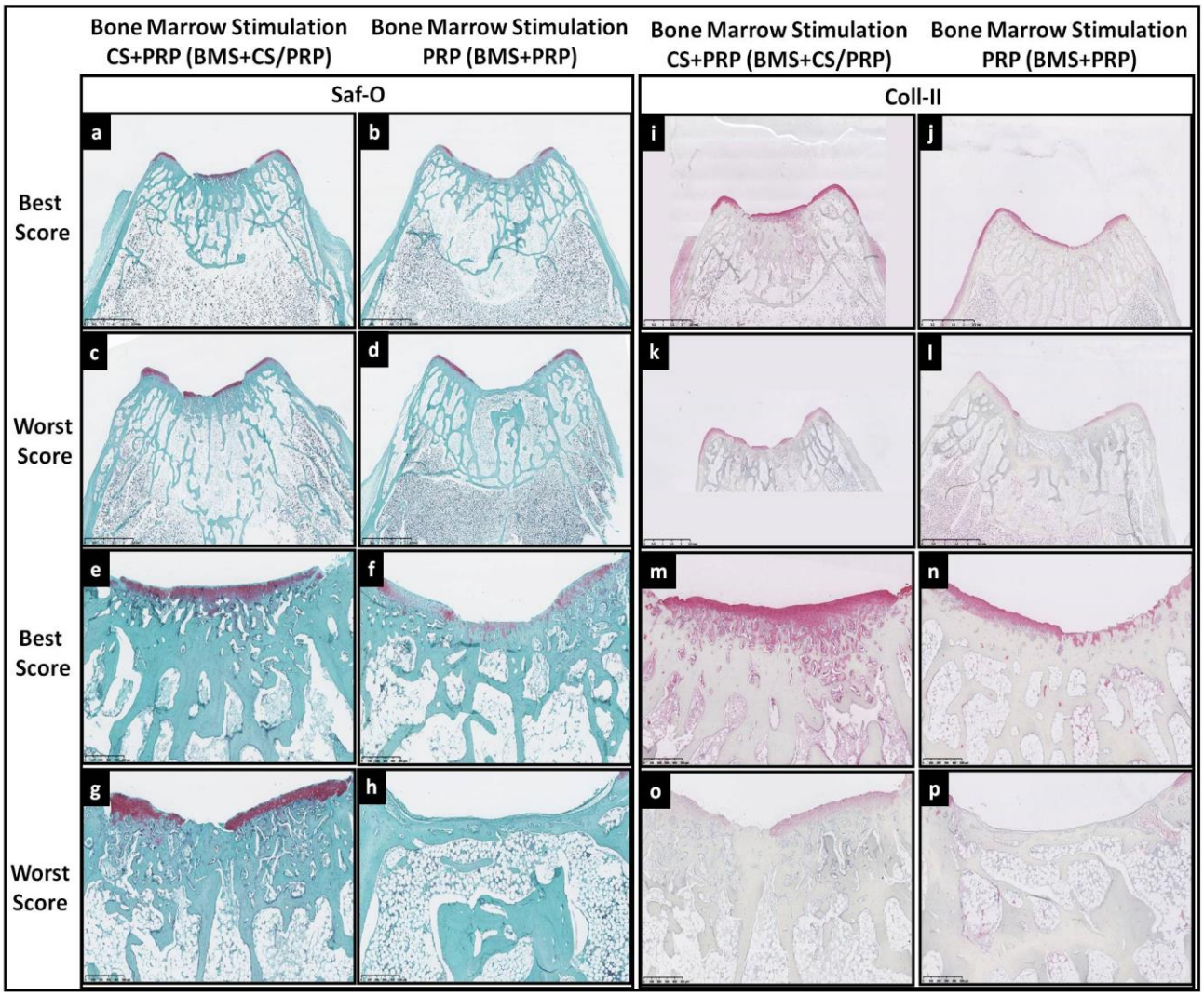

Fig. 4. Comparison of histopathological assessment of best and worst repair tissues generated by BMS+CS/PRP and BMS+PRP. **(a-h)**: Saf-O staining for best (a,b,e,f) and worst (c,d,g,h) repair outcomes; **(i-p):** Coll-II immunostaining for best (i,j,m,n) and worst (k,l,o,p) repair outcomes; Scale bars 2.5mm (a-d & i-l) and 500 µm (e-h & m-p).

Restoration of surface, structural integrity and thickness were all improved by BMS+CS/PRP treatment (p=0.05, p=0.0001 and p=0.002, respectively) [Fig.5 a,b,c,d] and [Fig.6 b]. Hypocellular tissue was less frequently observed in BMS+CS/PRP group and incidence of

chondrocyte clustering was more frequent in the BMS+PRP group (p=0.002 and p=0.009, respectively) [Fig.5 g,h,i,j] and [Fig.6 b]. Margins of defects were recognizable and degenerative changes were observed in the adjacent cartilage, especially in the BMS+PRP group (p=0.004) [Fig.5 e,f] and [Fig.6 b]. Zonal organization and tidemark were not restored in any defect at this 8 week time point [Fig.5 g,h,i,j]. One case of a cleft communicating with subchondral cyst was observed in both groups (Data not shown). Taken together, mean O'Driscoll score was significantly higher for BMS+CS/PRP group (Mean score 20.5±1.69) versus BMS+PRP group (Mean score 14.75±1.75) (p=0.0002), indicating superior quality of repair in presence of CS/PRP implants [Fig. 6a].

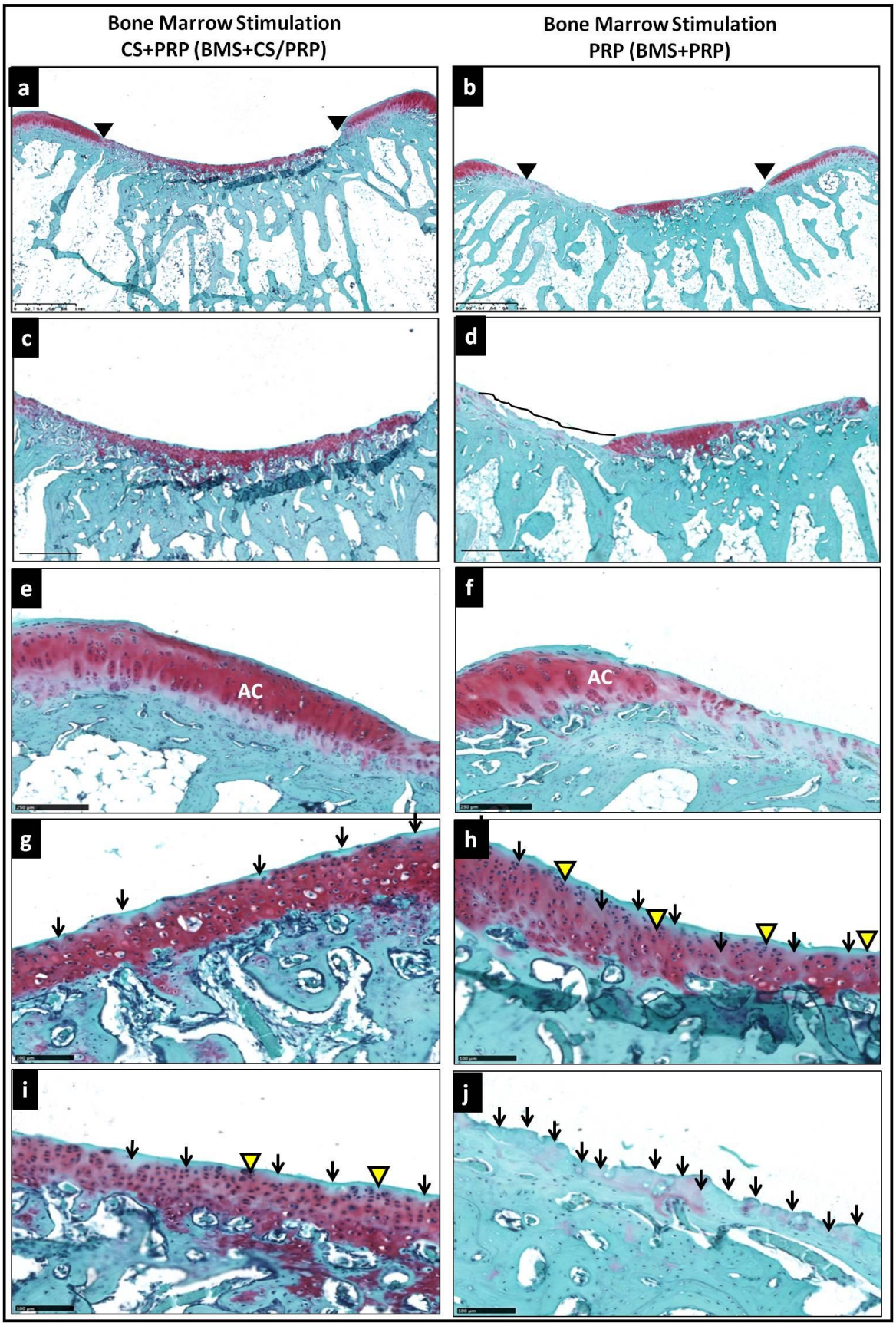
Bone Marrow Stimulation
CS+PRP (BMS+CS/PRP)
Bone Marrow Stimulation
PRP (BMS+PRP)
a
b
c
d
e
AC
f
AC
g
h
i
j

320

Fig. 5: Representative sections of repair tissues generated by BMS+CS/PRP and BMS+PRP. (a,b): Restoration of surface and structural integrity was better in presence of CS/PRP (a) versus PRP (b) (defect margins flanked by solid black arrows); (c,d): Missing repair tissue (line) in BMS+PRP (d) versus more uniform tissue in BMS+CS/PRP (c); (e,f): Comparison of adjacent cartilage (AC) showing improved appearance in the case of BMS+CS/PRP; (g,h): Best sections, (i,j): worst sections- all sections from same animal. Black arrows indicate zones of hypocellularity, yellow arrows indicate cell clusters, both more frequent in BMS+PRP. Scale bars=a,b: 1 mm, e-f: 250 µm, g-j: 100 µm.

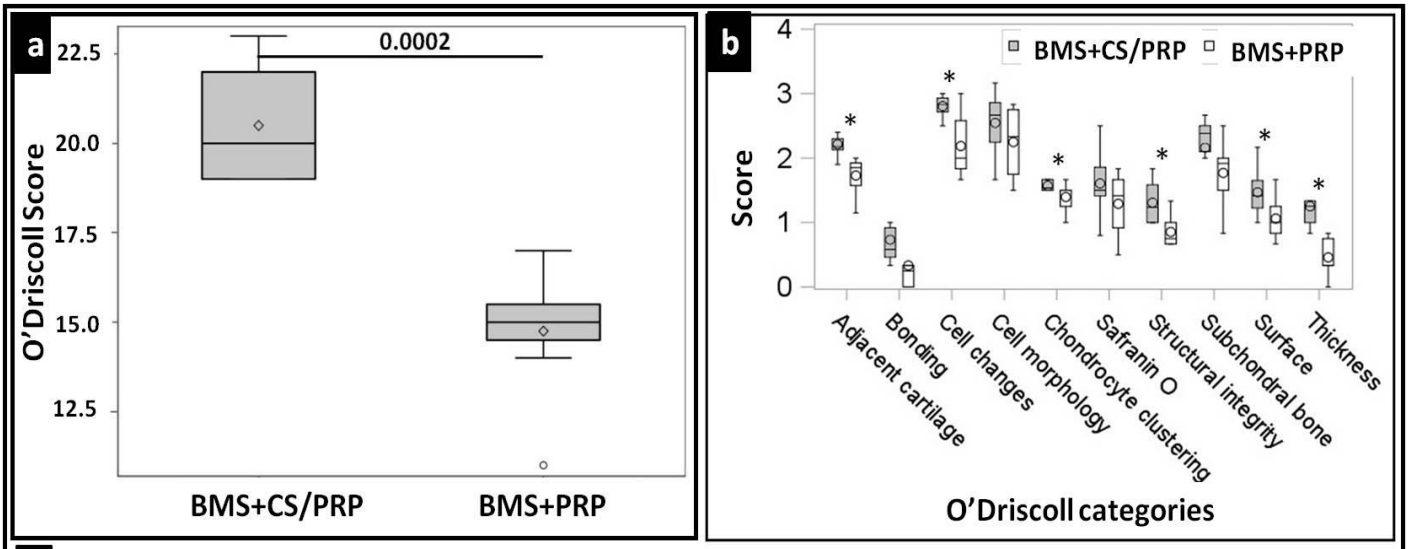

c

No.	Criteria	Score	No.	Criteria	Score
I	Chondrocyte Cell Morphology	0-4	VI	Bonding with adjacent cartilage	0-2
II	Saf-O staining	0-3	VII	Normal cellularity	0-3
III	Surface regularity	0-3	VIII	Chondrocyte clustering	0-2
IV	Structural integrity	0-2	IX	Degeneration in adjacent cartilage	0-3
V	Thickness	0-2	X	Subchondral bone health	0-3

Fig. 6: (a) Mean O'Driscoll score was significantly higher for repair tissues in defects treated with BMS+CS/PRP versus defects treated with BMS+PRP. (b). Significant differences (*) were observed between treatments, and scores for adjacent cartilage (p=0.004), cellular changes (p=0.002), cell clusters (p=0.009), structural integrity (p=0.0001), surface integrity (0.05) and thickness of repair tissue (p=0.002) were significantly higher for defects treated with BMS+CS/PRP. (c). Criteria used in modified O'Driscoll scoring with respective score range.

Quantitative histomorphometry revealed a significant increase in type II collagen staining in repair tissue matrix for BMS+CS/PRP group (Mean 57.37±12.43) compared to BMS+PRP group (Mean score 32±15.94), indicating a more hyaline repair (p=0.003) [Fig. 7a]. Safranin O staining was less widespread than type II collagen staining [Figs. 4,5,6]. A higher proportion of repair tissue was GAG-positive in the BMS+CS/PRP group (Mean 44.9±16.3) compared to BMS+PRP group (Mean 34.6±8.9), although this result was not significant (p=0.07) [Fig. 7b].

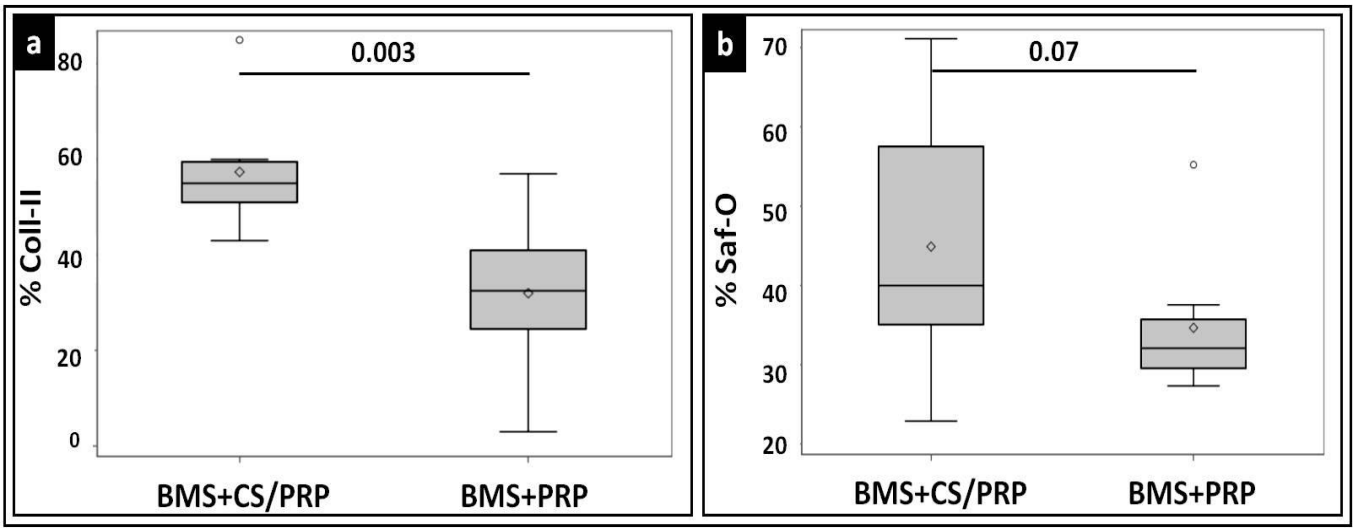

Fig. 7: a). Mean %Coll-II was significantly higher for repair tissues in defects treated with BMS+CS/PRP versus defects treated with BMS+PRP. **b).** Mean % Saf-O was higher for repair tissues in defects treated with BMS+CS/PRP versus defects treated with BMS+PRP, although this difference was not significant.

Chitosan/PRP implants induced bone remodeling in BMS-treated defects

In both groups at 8 weeks post-operative, subchondral bone underneath cartilage defects showed evidence of ongoing remodelling indicating repair was still underway [Fig. 4]. Quantitative 3-D micro CT analysis revealed high inter-individual variability in bone structural parameters, and no significant difference between treatments [Fig. 1S]. However, the values for bone surface density, bone surface, connectivity density, and trabecular number were all higher for BMS+CS/PRP group compared to BMS+PRP group (all p=0.01), indicating that CS/PRP implants increased bone remodeling [Fig. 1S].

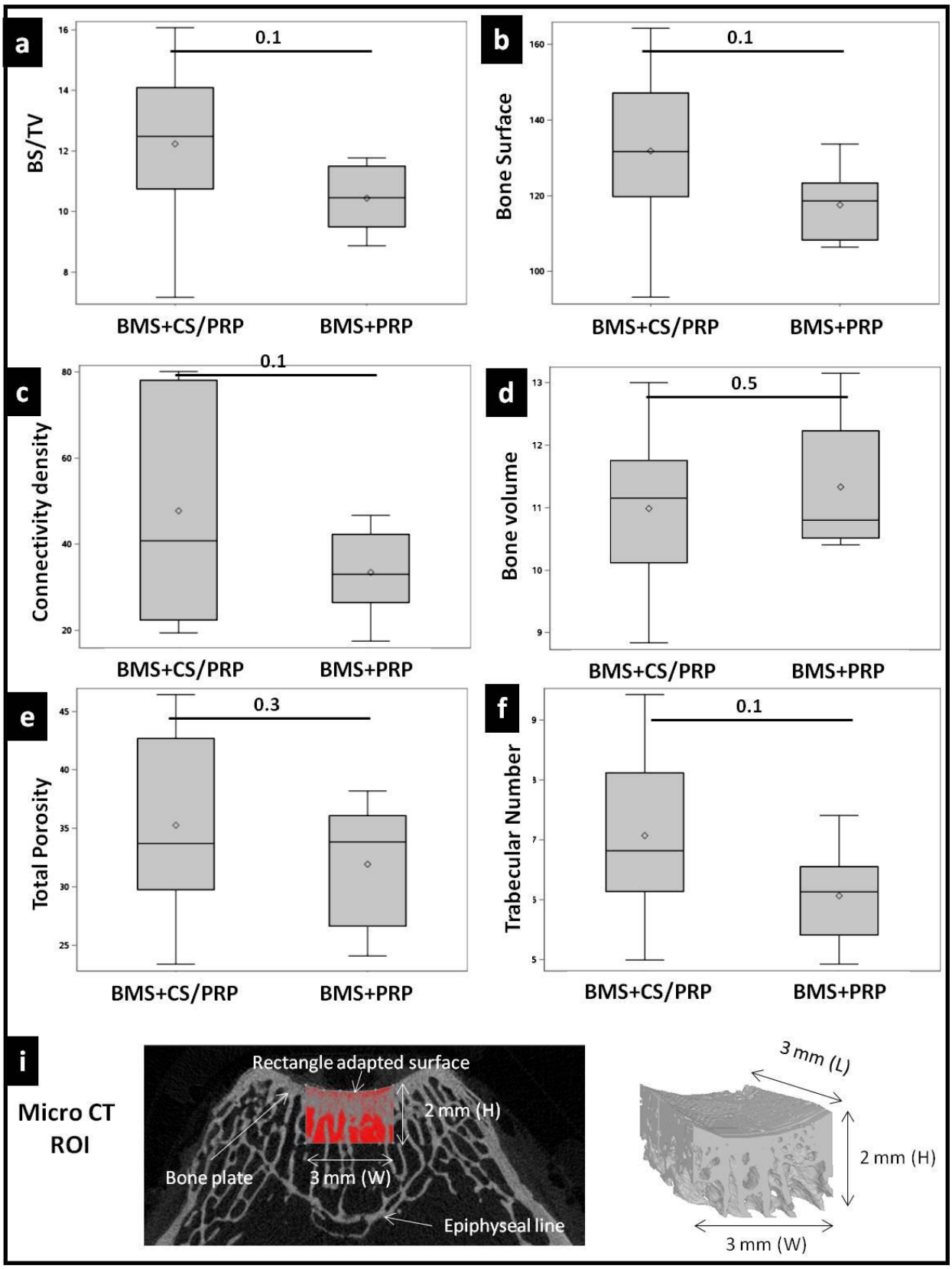
a
BS/TV
0.1
BMS+CS/PRP
BMS+PRP
b
Bone Surface
0.1
BMS+CS/PRP
BMS+PRP
c
Connectivity density
0.1
BMS+CS/PRP
BMS+PRP
d
Bone volume
0.5
BMS+CS/PRP
BMS+PRP
e
Total Porosity
0.3
BMS+CS/PRP
BMS+PRP
f
Trabecular Number
0.1
BMS+CS/PRP
BMS+PRP
i
Micro CT ROI
Rectangle adapted surface
2 mm (H)
Bone plate
3 mm (W)
Epiphyseal line
3 mm (L)
2 mm (H)
3 mm (W)

Fig. 1S: MicroCT 3-D analysis showed differences in structural parameters between defects treated with BMS+CS/PRP versus defects treated with BMS+PRP. Although the results were not significant, the values for bone surface density (a), bone surface (b), connectivity density (c), and trabecular number (f) were trending high for BMS+CS/PRP group versus BMS+PRP group, suggesting an increase in bone remodeling. i. Schematic representing the region of interest (ROI) for micro CT analysis.

Discussion

A chronic model was developed to test the efficacy of CS/PRP implants in augmenting marrow stimulated repair. Although chronic defects were found to be more challenging to treat than acute defects, CS/PRP implants improved the quality of repair tissues, which suggests that they would constitute a promising approach for treating chronic, degenerated lesions in older patients. Taken together, our data shows superiority of BMS+CS/PRP in repair of chronic defects compared to BMS+PRP, thereby affirming our starting hypothesis.

The chronic defect model used here was intended to approach the degenerative and inflammatory processes concomitant with metabolic alterations in early OA due to cartilage injury. In line with this, we found that BMS by drilling to 6 mm induced much poorer repair in trochlear chronic defects [Figs. 3,4] than in similar acute defects in the rabbit model [34,35]. Recent studies have reiterated the chronic defect model to be more suitable to study pathogenesis of OA which is associated with multiple changes in the defect milieu with severe bearing on downstream repair processes. Altered joint homeostasis in old defects has been associated with

inferior repair [40]. The difficulty in treating chronic defects has been recognized in multiple studies in the past [40,41]. Saris *et al* showed that cartilage repair outcome in groups receiving late treatment was significantly inferior compared to early treatment group and was comparable to untreated group [40]. Rodrigo *et al* suggested that synovial fluid may have a stimulatory effect in treatment of acute defects while may be inhibitory in chronic defect treatment [42].

PRP is a rich source of growth factors and cytokines which play important roles in inflammatory and wound repair phenomena [9,10]. Although the exact mechanism of PRP action has not been understood, BMSC recruitment, expression of cartilage matrix [18] in addition to migration, proliferation and chondrogenesis of subchondral BMSCs have been shown to be positively influenced by PRP. In contrast, some studies report that PRP exerts a stimulatory effect on proliferation of chondrocytes and BMSCs, but has no effect on their chondrogenic differentiation [17, 47-49]. Reduced expression of lineage specific markers was observed in cells expanded in the presence of PRP [50]. Therefore, we believe that BMS augmented with recalcified PRP was an appropriate baseline treatment to be compared with BMS repair outcome elicited in presence of CS/PRP implants. Our results indicate insufficient capability of PRP in enabling cartilage healing in a chronic defect [Figs. 3,4,5,6,7]. Similarly, in a previously published study, PRP was unsuccessful in regenerating the hyaline nature of repair tissue in a chronic defect treated with BMS [18]. In our study, PRP failed to solidify even after several minutes in most cases, suggesting impaired *in vivo* residency of a liquid implant, and providing a possible mechanism for reduced efficacy of PRP in cartilage regeneration. In our recent study, CS/PRP clots showed significant increase in viscosity vs PRP and reduced clotting time by 4 times compared to recalcified PRP [23]. Whereas CS/PRP clots remained voluminous even 1

hour after clotting, recalcified PRP clots had lost ~80% of their original volume as a result of serum exudation [23]. The resulting quick loss of platelet-derived bioactive factors could potentially limit repair in these defects. In our implants, CS inhibited the retraction observed in PRP clots and solid, voluminous CS/PRP implants increased stability *in vivo*, ensuring bioactivity for several weeks. Consistent with this hypothesis, CS/PRP implants have been shown to reside for several weeks *in vivo* and to possess significant bioactivity while recalcified PRP degraded in a day [23]. In addition, when implanted subcutaneously, the sustained presence of CS/PRP implants induced cell recruitment and angiogenesis in the local milieu. A similar increase in recruitment of progenitor cells combined with increased angiogenesis will greatly influence the cartilage tissue regeneration and subchondral bone remodeling. Possibly through platelet activation, CS increases the concentration of bioactive factors including proangiogenic factors [61]. Our own in-house preliminary data [62] and other studies suggest that CS may stabilize platelets in PRP leading to sustained release of GFs [58]. Kim *et al* had shown improved chondrocyte proliferation and matrix synthesis induced by sustained release of TGF-βI from CS scaffolds [63]. Taken together, we believe that superior physical stability of CS/PRP implants leads to a significant increase in their biological activity arising from sustained residency and release of platelet-derived growth factors and inherent benefits of CS.

Potentiating effects of CS in articular cartilage healing has been demonstrated in multiple studies [51-54]. While CS helped in maintenance of morphology and ECM synthesis by chondrocytes *in vitro* [53,54], a thermosensitive CS gel promoted chondrogenic differentiation of BMSCs [55]. CS has been shown to be chemotactic and increase recruitment and proliferation of BMSCs into defect [4], impede loss and preserve viability of BMSCs [56]. Three-week analysis

of repair tissues in our model revealed the presence of vascularized granulation tissue enriched with polymorphonuclear cells along with enlarged drill holes in CS/PRP group, similar to what was previously reported for CS-GP/blood implants [4,57]. In contrast, a typical fibrocartilagenous repair and endochondral ossification associated with hypertrophied chondrocytes and vascular invasion was observed in BMS only group, as previously reported [1, 4]. CS-GP/blood implants improve cartilage repair by, in part, increasing cell recruitment, vascularization and bone remodeling, polarizing the macrophage phenotype towards the alternatively-activated pro-wound healing lineage and stimulating secretion of anabolic wound repair factors [4, 5, 58-60]. Wound bloom effect as seen in previous studies was characterized by enhanced woven bone plate repair in the drill holes along with increase in volume and hyaline quality of cartilage tissue, likely due to increased recruitment of chondrogenic stem cells to the cartilage lesion [57]. Here, we showed that CS/PRP implants appear to induce similar mechanisms. Taken together, these factors may drive the superior repair response in presence of CS/PRP implants indicated by more hyaline nature of repair accompanied by better macroscopic regeneration and increased bone remodeling.

One limitation of this study was its relatively short 8 week time point. Although increased hyaline nature of the repair tissue obtained with BMS+CS/PRP would be expected to provide long-term durability, this was not assessed here. In addition, we found high inter-individual variability in our results, which may arise due to immediate load bearing [64] further compounded by small sample size used in this study. Nevertheless, in spite of these limitations, CS/PRP implants show promise in augmenting the beneficial effects of BMS in chronic models.

Conclusions

We believe that this study will motivate earnest reassessment of pre-clinical cartilage repair models. Since prompt diagnosis and treatment of cartilage defects is rare, approaches aimed at improving repair in presence of altered joint hemostasis is warranted. The chronic model studied here is more comparable to human chronic defects than the corresponding acute model. Our results show promising results in unveiling the positive role of CS/PRP implants for improvement of BMS mediated cartilage repair in chronic defects. In the future, a larger study with increased duration of repair and additional control groups will be undertaken to shed more light on the underlying mechanism of inflammatory and metabolic changes accompanying pathogenesis and repair of chronic defects using CS/PRP implants.

Acknowledgments

We acknowledge the technical contributions of Jun Sun and Geneviève Picard. This work was supported by the Canadian Institutes of Health Research, Canada Foundation for Innovation, Groupe de Recherche en Sciences et Technologies Biomédicales, Natural Sciences and Engineering Research Council of Canada and Ortho Regenerative Technologies Inc.

Declaration of interest

AC, CDH and MDB hold shares and CDH and MDB are Directors of Ortho Regenerative Technologies Inc.

References

1) F. Shapiro F, S. Koide, M.J. Glimcher, Cell origin and differentiation in the repair of full-thickness defects of articular cartilage, The Journal of bone and joint surgery. American volume 75(4) (1993) 532-53.
2) C.D. Hoemann, J. Sun, M.D. McKee, A. Chevrier, E. Rossomacha, G.E. Rivard, M. Hurtig, M.D. Buschmann, Chitosan-glycerol phosphate/blood implants elicit hyaline cartilage repair integrated with porous subchondral bone in microdrilled rabbit defects, Osteoarthritis and Cartilage 15(1) (2007) 78-89.
3) C.D. Hoemann, M. Hurtig, E. Rossomacha, J. Sun, A. Chevrier, M. Shive, M. Buschmann, Chitosan-glycerol phosphate/blood implants improve hyaline cartilage repair in ovine microfracture defects, Journal of Bone and Joint Surgery-American Volume 87A(12) (2005) 2671-2686.
4) A Chevrier, C.D. Hoemann, J. Sun, M.D. Buschmann, Chitosan-glycerol phosphate/blood implants increase cell recruitment, transient vascularization and subchondral bone remodeling in drilled cartilage defects, Osteoarthritis and Cartilage 15(3) (2007) 316-327.
5) G. Chen, J. Sun, V. Lascau-Coman, A. Chevrier, C. Marchand, C.D. Hoemann, Acute Osteoclast Activity following Subchondral Drilling Is Promoted by Chitosan and Associated with Improved Cartilage Repair Tissue Integration, Cartilage 2(2) (2011) 173-185.
6) W.D. Stanish, R.G. McCormack, F. Forriol, N. Mohtadi, S. Pelet, J. Desnoyers, A. Restrepo, M.S. Shive, Novel Scaffold-Based BST-CarGel Treatment Results in Superior

Cartilage Repair Compared with Microfracture in a Randomized Controlled Trial, Journal of Bone and Joint Surgery-American Volume 95A(18) (2013) 1640-1650.

7) M.S. Shive, W.D. Stanish, R. McCormack, F. Forriol, N. Mohtadi, S. Pelet, J. Desnoyers, S. Methot, K. Vehik, A. Restrepo, BST-CarGel(R) Treatment Maintains Cartilage Repair Superiority over Microfracture at 5 Years in a Multicenter Randomized Controlled Trial, Cartilage 6(2) (2015) 62-72.

8) K.M. Varum, M.H. Ottoy, O. Smidsrod, Acid hydrolysis of chitosans, Carbohydrate Polymers 46(1) (2001) 89-98.

9) Marx RE, Carlson ER, Eichstaedt RM, Schimmele SR, Strauss JE, Georgeff KR. Platelet-rich plasma: Growth factor enhancement for bone grafts. Oral surgery, oral medicine, oral pathology, oral radiology, and endodontics; (1998). 85: 638-646.

10) Gonshor A. Technique for producing platelet-rich plasma and platelet concentrate: background and process. The International journal of periodontics & restorative dentistry. (2002). 22: 547-557.

11) Marx RE. Platelet-rich plasma (PRP): what is PRP and what is not PRP? Implant dentistry; (2001). 10: 225-228

12) Simpson AHRW, Mills L, Noble B. (2006). The role of growth factors and related agents in accelerating fracture healing. J Bone Joint Surg Br. 88:701–5.

13) Veillette CJ, McKee MD. Growth factors—BMPs, DBMS, and buffy coat products: are there any proven differences amongst them? Injury. (2007). 38: S38–48

14) Smyth NA, Murawski CD, Fortier LD, Cole BJ, Kennedy JG. Platelet-Rich Plasma in the Pathologic Processes of Cartilage:Review of Basic Science Evidence. Arthroscopy: The Journal of Arthroscopic and Related Surgery. (2013). 29:8, 1399-1409.

15) Lee H, Park KM, Park KD, Joung YK, Do Hee S Platelet-rich plasma loaded hydrogel scaffold enhances chondrogenic differentiation and maturation with upregulation of CB1 and CB2. J Control Release. (2012). 159:332-337.

16) Park SI, Lee HR, Kim S, Ahn MW, Do SH. Time-sequential modulation in expression of growth factors from platelet-rich plasma (PRP) on the chondrocyte cultures. Mol Cell Biochem, (2012). 361:9-17.

17) Krüger JP, Hondke S, Endres M, Pruss A, Siclari A,Kaps C. Human platelet-rich plasma stimulates migration and chondrogenic differentiation of human subchondral progenitor cells. J Orthop Res. (2012). 30:845-852.

18) G. Milano, E. Sanna Passino, L. Deriu, G. Careddu, L. Manunta, A. Manunta, M.F. Saccomanno, C. Fabbriciani, The effect of platelet rich plasma combined with microfractures on the treatment of chondral defects: an experimental study in a sheep model, Osteoarthritis and cartilage 18(7) (2010) 971-80.

19) W. Brehm, B. Aklin, T. Yamashita, F. Rieser, T. Trub, R.P. Jakob, P. Mainil-Varlet, Repair of superficial osteochondral defects with an autologous scaffold-free cartilage construct in a caprine model: implantation method and short-term results, Osteoarthritis and Cartilage 14(12) (2006) 1214-1226.

20) E. Kon, G. Filardo, M. Delcogliano, M. Fini, F. Salamanna, G. Giavaresi, I. Martin, M. Marcacci, Platelet autologous growth factors decrease the osteochondral regeneration capability of a collagen-hydroxyapatite scaffold in a sheep model, BMC musculoskeletal disorders 11 (2010b).

21) H.-R. Lee, K.M. Park, Y.K. Joung, K.D. Park, S.H. Do, Platelet-rich plasma loaded hydrogel scaffold enhances chondrogenic differentiation and maturation with up-regulation of CB1 and CB2, Journal of Controlled Release 159(3) (2012) 332-337.

22) C.J.A. van Bergen, G.M.M.J. Kerkhoffs, M. Ozdernir, e. al., Demineralized bone matrix and platelet-rich plasma do not improve healing of osteochondral defects of the talus: an experimental goat study, Osteoarthritis and Cartilage 21(11) (2013) 1746-1754.

23) A. Chevrier, V. Darras, G. Picard, M. Nelea, D. Veilleux, M. Lavertu, C.D. Hoemann, M.D. Buschmann, Injectable chitosan-platelet-rich plasma (PRP) implants to promote tissue regeneration: In vitro properties, in vivo residence, degradation, cell recruitment and vascularization, tissue Engineering and Regenerative Medicine In Press (2016).

24) Bredella MA, Tirman PF, Peterfy CG, Zarlingo M, Feller JF, Bost FW, Belzer JP, Wischer TK, Genant HK. Accuracy of T2-weighted fast spin-echo MR imaging with fat saturation in detecting cartilage defects in the knee: comparison with arthroscopy in 130 patients. AJR Am J Roentgenol. (1999); 172:1073–1080.

25) Hardaker WT Jr, Garrett WE Jr, Bassett FH 3rd. Evaluation of acute traumatic hemarthrosis of the knee joint. South Med J. (1990);83:640–644.

26) Bouwmeester SJ, Kuijer R, Homminga GN, Bulstra SK, Geesink RG. A retrospective analysis of two independent prospective cartilage repair studies: autogenous perichondrial grafting versus subchondral drilling 10 years post-surgery. J Orthop Res. (2002);20:267–273.

27) Bouwmeester SJ, Kuijer R, Terwindt-Rouwenhorst EA, van der Linden AJ, Bulstra SK. Histological and biochemical evaluation of perichondrial transplants in human articular cartilage defects. J Orthop Res. (1999);17:843–849.

28) Hunziker EB. Biologic repair of articular cartilage: defect models in experimental animals and matrix requirements. Clin Orthop Relat Res. [1999];367(suppl):S135–S146.

29) Mizuta H, Kudo S, Nakamura E, Takagi K, Hiraki Y. Expression of the PTH/PTHrP receptor in chondrogenic cells during the repair of full-thickness defects of articular cartilage. Osteoarthritis Cartilage. (2006);14:944–952.

30) Harada Y, Nakasa T, Mahmoud EE, Kamei G, Adachi N, Deie M, OchiM. Combination Therapy With Intra-Articular Injection of Mesenchymal Stem Cells and Articulated Joint Distraction for Repair of a Chronic Osteochondral Defect in the Rabbit. J Orthop Res (2015). 33:1466–1473.

31) Hepp P, Osterhoff G, Niederhagen M, Marquass B, Aigner T, Bader A, Josten C, Schulz R. Perilesional changes of focal osteochondral defects in an ovine model and their relevance to human osteochondral injuries. J Bone Joint Surg [Br] (2009);91-B:1110-19.

32) M. Lavertu, Z. Xia, A.N. Serreqi, M. Berrada, A. Rodrigues, D. Wang, M.D. Buschmann, A. Gupta, A validated 1H NMR method for the determination of the degree of deacetylation of chitosan, J Pharm Biomed Anal 32(6) (2003) 1149-58

33) S. Nguyen, F.M. Winnik, M.D. Buschmann, Improved reproducibility in the determination of the molecular weight of chitosan by analytical size exclusion chromatography, Carbohydrate Polymers 75(3) (2009) 528-533.

34) H. Chen, C.D. Hoemann, J. Sun, A. Chevrier, M.D. McKee, M.S. Shive, M. Hurtig, M.D. Buschmann, Depth of Subchondral Perforation Influences the Outcome of Bone Marrow Stimulation Cartilage Repair, Journal of Orthopaedic Research 29(8) (2011) 1178-1184.

35) H. Chen, A. Chevrier, C.D. Hoemann, J. Sun, G. Picard, M.D. Buschmann, Bone Marrow Stimulation of the Medial Femoral Condyle Produces Inferior Cartilage and Bone Repair Compared to the Trochlea in a Rabbit Surgical Model, Journal of Orthopaedic Research 31(11) (2013) 1757-1764.

36) H. Chen, J. Sun, C.D. Hoemann, V. Lascau-Coman, O. Wei, M.D. McKee, M.S. Shive, M.D. Buschmann, Drilling and Microfracture Lead to Different Bone Structure and Necrosis during Bone-Marrow Stimulation for Cartilage Repair, Journal of Orthopaedic Research 27(11) (2009) 1432-1438.

37) M.P. van den Borne, N.J. Raijmakers, J. Vanlauwe, J. Victor, S.N. de Jong, J. Bellemans, D.B. Saris, International Cartilage Repair Society (ICRS) and Oswestry macroscopic cartilage evaluation scores validated for use in Autologous Chondrocyte Implantation (ACI) and microfracture, Osteoarthritis and cartilage / OARS, Osteoarthritis Research Society 15(12) (2007) 1397-402

38) C.D. Hoemann, N. Tran-Khanh, A. Chevrier, G. Chen, V. Lascau-Coman, C. Mathieu, A. Changoor, A. Yaroshinsky, R.G. McCormack, W.D. Stanish, M.D. Buschmann, Chondroinduction Is the Main Cartilage Repair Response to Microfracture and Microfracture With BST-CarGel: Results as Shown by ICRS-II Histological Scoring and a Novel Zonal Collagen Type Scoring Method of Human Clinical Biopsy Specimens, The American journal of sports medicine 43(10) (2015) 2469-80**.**

39) C. Marchand, H. Chen, M.D. Buschmann, C.D. Hoemann, Standardized Three-Dimensional Volumes of Interest with Adapted Surfaces for More Precise Subchondral Bone Analyses by Micro-Computed Tomography, Tissue Engineering Part C-Methods 17(4) (2011) 475-484.

40) Saris DB, Dhert WJ, Verbout AJ. Joint homeostasis: the discrepancy between old and fresh defects in cartilage repair. J Bone Joint Surg [Br] (2003);85-B:1067-76.

41) Verbruggen G, Wittoek R, Groenboer S, et al. Osteochondral repair in synovial joints. Curr Opin Rheumatol 2007;19:265-71.

42) Rodrigo JJ, Steadman JR, Syftestad G, Benton H, Silliman J. Effects of human knee synovial fluid on chondrogenesis in vitro. Am J Knee Surg (1995);8:124-9.

43) Nam J, Perera P, Liu J., Sequential alterations in catabolic and anabolic gene expression parallel pathological changes during progression of monoiodoacetate-induced arthritis. PLoS ONE, (2011) 6, no. 9,Article ID e24320.

44) Goldring MB, Goldring SR. Articular cartilage and subchondral bone in the pathogenesis of osteoarthritis. Annals of theNew York Academy of Sciences, (2010) 1192: 230–237.

45) van der Kraan PM, van den Berg WB. Osteophytes: relevance and biology. Osteoarthritis and Cartilage, (2007) vol. 15, no. 3, pp. 237–244.

46) Dorotka R, Windberger U, Macfelds K, et al. Repair of articular cartilage defects treated by microfracture and a three-dimensional collagen matrix. Biomaterials (2005);26:3617-29.

47) Kaps C, Loch A, Haisch A. Human platelet supernatant promotes proliferation but not differentiation of articular chondrocytes. Med Biol Eng Comput (2002) 40:485–490.

48) Gaissmaier C, Fritz J, Krackhardt T, et al. Effect of human platelet supernatant on proliferation and matrix synthesis of human articular chondrocytes in monolayer and three-dimensional alginate cultures. Biomaterials (2005) 26:1953– 1960.

49) Drengk A, Zapf A, Sturmer EK. Influence of platelet-rich plasma on chondrogenic differentiation and proliferation of chondrocytes and mesenchymal stem cells. Cells Tissues Organs (2009)189:317–326.

50) Li H, Usas A, Poddar M, Chen C, Thompson S, Ahani B, Cummins J, Lavasani M, Huard J. Platelet-Rich Plasma Promotes the Proliferation of Human Muscle Derived Progenitor Cells and Maintains Their Stemness. PLoS ONE (2013) 8(6): e64923.

51) Lu JX, Prudhommeaux F, Meunier A, Sedel L, Guillemin G. E!ects of chitosan on rat knee cartilages. Biomaterials (1999);20(20):1937-44.

52) Mattioli-Belmonte M, Gigante A, Muzzarelli RA, Politano R, De Benedittis A, Specchia N, Bu!a A, Biagini G, Greco F. N,Ndicarboxymethyl chitosan as delivery agent for bone morphogenetic
protein in the repair of articular cartilage. Med Biol Eng Comput (1999);37(1):130-4.

53) Risbud M, Ringe J, Bhonde R, Sittinger M. In vitro expression of cartilage-specific markers by chondrocytes on a biocompatible hydrogel: implications for engineering cartilage tissue. Cell
Transplant (2001);10:755–63.

54) Hsu SH, Whu SW, Hsieh SC, Tsai CL, Chen DC, Tan TS. Evaluation of chitosan–algin ate–hyaluronate complexes modified by an RGD-containing protein as tissue-engineering scaffolds for cartilage regeneration. ArtifOrg (2004);28:693–703

55) Cho JH, Kim SH, Park KD, et al. Chondrogenic differentiation of human mesenchymal stem cells using a thermosensitive poly(N-isopropylacrylamide) and water-soluble chitosan copolymer. Biomaterials (2004);25:5743.

56) Alberto Busilacchi A, Gigante A, Mattioli-Belmonte M, Manzotti S, Muzzarelli R AA. Chitosan stabilizes platelet growth factors and modulates stem cell differentiation toward tissue regeneration. Carbohydrate Polymers 98 (2013) 665– 676.

57) J. Guzman-Morales, C.H. Lafantaisie-Favreau, G. Chen, C.D. Hoemann, Subchondral chitosan/blood implant-guided bone plate resorption and woven bone repair is coupled to hyaline cartilage regeneration from microdrill holes in aged rabbit knees, Osteoarthritis and Cartilage 22(2) (2014) 323-333.

58) C.D. Hoemann, G. Chen, C. Marchand, N. Tran-Khanh, M. Thibault, A. Chevrier, J. Sun, M.S. Shive, M.J.G. Fernandes, P.E. Poubelle, M. Centola, H. El-Gabalawy, Scaffold-Guided Subchondral Bone Repair Implication of Neutrophils and Alternatively Activated Arginase-1+Macrophages, American Journal of Sports Medicine 38(9) (2010) 1845-1856.

59) D. Fong, M.B. Ariganello, J. Girard-Lauziere, C.D. Hoemann, Biodegradable chitosan microparticles induce delayed STAT-1 activation and lead to distinct cytokine responses in differentially polarized human macrophages in vitro, Acta biomaterialia 12 (2015) 183-94.

60) Fischer, T. H., Thatte, H. S., Nichols, T. C., Bender-Neal, D. E., Bellinger, D. A., Vournakis, J. N. Synergistic platelet integrin signaling and factor XII activation in poly-N-acetyl glucosamine fiber-mediated hemostasis. Biomaterials, (2005). 26: 5433–5443

61) G. Deprés-Tremblay, A. Chevrier, N. Tran-Khanh, M. Nelea, M.D. Buschmann, Chitosan-platelet-rich plasma implants for tissue repair - in vitro and in vivo characteristics, World Biomaterials Congress, Montreal, QC, Canada, 2016.

62) Lee JY, Nam SH, Im SY, Park YJ, Lee YM, Seol YJ, Chung CP, Lee SJ. Enhanced bone formation by controlled growth factor delivery from chitosan-based biomaterials. J Control Release (2002);78:187–97.

63) Suh JKF, Matthew HWT. Application of chitosan-based polysaccharide biomaterials in cartilage tissue engineering: a review. Biomaterials (2000) 21: 2589-2598.

64) Jubel A, Andermahr J, Schiffer G, Rehm KE, Stoddart MJ, Hauselmann HJ. Transplantation of de novo scaffold-free cartilage implants into sheep knee chondral defects. Am J Sports Med. (2008); 36(8):1555-1564.